Semnan University

Journal of Heat and Mass Transfer Research

Journal homepage: http://jhmtr.journals.semnan.ac.ir

Heat Transfer Studies of Supercritical Water Flows in an Upward Vertical Tube

S. Anand[a], S. Suresh[b], D. Santhosh Kumar [a,*]

[a] *Bharat Heavy Electricals Limited, Trichy.*
[b] *Department of Mechanical Engineering, NIT-Trichy*

PAPER INFO

Paper history:
Received: 2019-04-16
Received: 2019-09-07
Accepted: 2019-09-24

Keywords:
Supercritical water;
heat transfer deterioration;
SST-kw model;
heat transfer enhancement;
vertical flow.

ABSTRACT

In this paper, an investigation of heat transfer characteristics at supercritical pressure fluid flowing in a uniformly heated vertical tube has been carried out. In order to reduce thermal emissions and increase thermal efficiency, supercritical boilers were developed at various sizes. Above supercritical pressure, the distinction of liquid and gas phases disappears. This dispenses with the problem of critical heat flux and dry out phenomenon which occurs in subcritical pressure. However, the study of heat transfer behavior above supercritical pressure is indeed required due to the heat transfer deterioration operation at high heat flux to mass flux ratio. In the present work, numerical simulation has been employed in order to inquire about the effect of various parameters such as heat flux to mass flux ratio, diameter and pressure that causes heat transfer deterioration. Shear Stress Transport k-ω model has been applied in all the computations. It is observed that the metal temperature predicted by numerical simulation is more accurate than the empirical correlations available in the literature. A Visual Basic Program has also been developed to assess the empirical correlations in the context of predicting metal temperature under 5280 different operating conditions. Tube sizes of 10, 15 & 20 mm inner diameter with 4 m length, the pressure between 225 and 280 bar and heat flux to mass flux ratio between 0.27 and 0.67 have been chosen to explore the effect of diameter, pressure and heat flux respectively.

DOI: 10.22075/jhmtr.2019.17488.1229

1. Introduction

Supercritical fluids play a critical role in various fields such as power plant engineering, aerospace engineering, chemical engineering and refrigeration engineering. Supercritical Carbon-dioxide is applied in the new generation of air-conditioning, refrigeration systems, compact air coolers and heat exchangers. Almost for a decade, supercritical technology is the most promising technology in both coal-fired and nuclear power plant applications. The change which occurred in the operating pressure of coal-fired plants from subcritical to supercritical enlarges the thermal efficiency of the power plant from 33% to 48 % which consequently reduces coal consumption. The Generation IV International Forum [1] recommends the Supercritical pressure water-cooled reactor concepts as one of the six promising reactor concepts. For the past few decades, several investigations are being employed in order to interpret the heat transfer behavior of Supercritical (SC) fluids [2-4].

There are three types of heat transfer modes such as Normal Heat Transfer (NHT), Heat Transfer Enhancement (HTE) and Heat Transfer Deterioration (HTD) occurring in forced convective supercritical heat transfer [5]. In Normal heat transfer mode, the Heat Transfer Coefficient (HTC) is no different compared to those of convective heat transfer that occurs far away from the pseudocritical regime at the subcritical condition and closely matches with the HTC computed applying Dittus-Boelter equation Eq. (1). In the reinforced heat transfer, the measured HTC are higher than those of normal HTC and consequently results in lower wall temperature near pseudocritical regimes. In heat transfer deterioration (HTD), the

* *Corresponding Author: D. Santhosh Kumar, Bharat Heavy Electricals Limited, Trichy.*
Email: santhoshkumar@bhel.in

measured HTC is lower of normal HTC and results in higher wall temperature near pseudocritical regimes.

$$Nu = 0.0243\,Re^{0.8}Pr^{0.4} \quad (1)$$

Wang et al. [6] depicted that the sudden changes of thermo-physical properties of supercritical water near pseudo-critical points are the major cause for changes in heat transfer. Unlike subcritical conditions, the thermo-physical properties of water such as specific heat, density, thermal conductivity and viscosity drastically change near pseudo-critical temperature and there is no distinguishable phase between liquid and vapor. Fig. 1 [7] exhibits the drastic change in thermo-physical properties of water when it reaches the pseudo critical point at 255 bar pressure. Wang et al. [6] and Cheng et al. [8] stated that the heat transfer deterioration (HTD) at supercritical conditions should be prevented in power plants due to its operation of raising the wall temperature abruptly and exceeding the maximum allowable value of the material as well as making the tube puncture. They also mentioned that the reinforced and deteriorated heat transfer occurs at low and high values of heat flux respectively. Duffey et al. [9] make the process by explaining that heat transfer deterioration takes place by two mechanisms, one is the sudden decrease of heat transfer coefficient (HTC) and the other is the sharp increase of wall temperature. Former is due to high heat flux to mass flux ratio and the latter is due to the formation of pseudo-film boiling on the tube surface. The HTD arises only at a small part of the tubes where the fluid temperature is near pseudo-critical temperature. Nevertheless, the occurrence of HTD not only depends on the fluid temperature near pseudocritical temperature but also on heat flux to mass flux ratio, the diameter of the tube and pressure. Moreover, the phenomenon of heat transfer deterioration is observed by Koshizuka et al. [10], Mokry et al. [11], Wen and Gu [12], Shen et al. [13], Anand et al. [14-15]. Pursuant to their observation, the HTD is mainly affected by the mass flux and the heat flux. Yamagata et al. [16] concluded that the critical heat flux causes HTD by the following formulae.

$$q_{c=}0.2G^{1.2} \quad (2)$$

They experimentally verified that HTD occurs above the limit heat flux related to the mass flux in a 10 mm diameter tube at pressures of 226-294 bar. Ackerman et al. [17] discussed that during pseudo film boiling, low-density layer forms near the wall which covers the tube surface as a blanket to retard the high-density water from touching the heated tube. They also demonstrated that a boiling like noise at the onset of heat transfer deterioration is being generated. Consequently, a similar phenomenon like a boiling crisis under sub-critical pressures could be presumed for supercritical pressures region. They came to the conclusion that the heat transfer deterioration point moves towards the downstream of the tube by increasing pressure, increasing mass flux and decreasing tube diameter. They depicted that there is a considerable increase in allowable heat flux against decreasing the tube diameter.

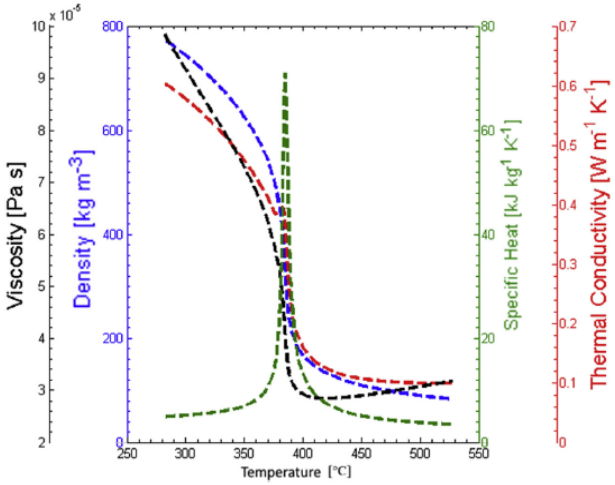

Figure 1. Thermo-physical properties of water near the pseudo-critical point at 255 bar pressure [7]

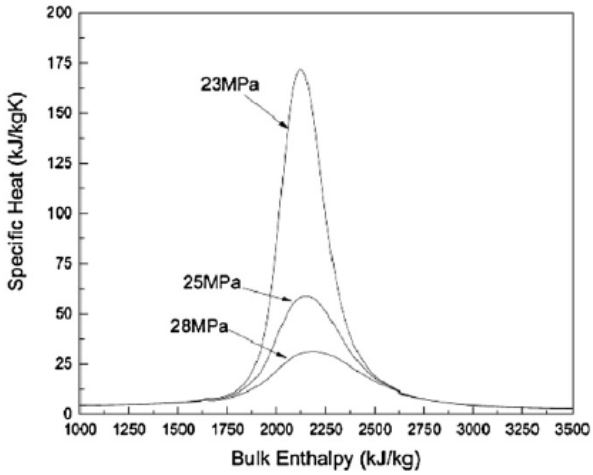

Figure 2. Specific heat variation at various pressures [25]

In 1974, Lee and Haller et al. [18] observed that besides high heat flux, the tube diameter is one of the key factors for HTD as well. Furthermore,they proposed mass velocity limits for the onset of HTD for given heat flux and tube diameter for fluid temperature below the pseudocritical temperature. Song et al. [19] mentioned that larger diameter tubes get affected by HTD as a result of the buoyancy effect. Watts and Chou et al. [20] proposed a Nusselt number correlation, in 1982, at the HTD regime, whose trend is that HTC is inversely proportional to the diameter of the tube. Yamashita et al. [21] correlated the limit heat flux and the bulk fluid enthalpy with tube diameter and also graphically represented that limit heat flux is larger at a small diameter for the onset of HTD. Another parameter which influences HTD is buoyancy (Bu) defined as follows by [22]

$$Bu = \overline{Gr_b} / Re^{2.7} \quad (3)$$

$$\overline{Gr_b} = (\rho_b\,(\rho_b - \rho)g\,d^3)/\mu_b^2 \quad (4)$$

$$Re_b = Gd/\mu_b \quad (5)$$

which indicates Bu α d0.3. Consequently, the Onset of HTD in larger diameter tubes is a result of the increase in buoyancy parameter (i.e., increase in free convection) as reported by Jackson and Haller 2003 [22] and Bae et al. [23]. Strong buoyancy effect transpired in larger diameters and it will lead to deteriorated heat transfer. In 2014, Yildiz et al. [24] assessed the effect of diameter based on a literature review and concluded that the effect of diameter on HTD is less clear. Although there appears to be some preference for a decrease in HTC with an increase in diameter, some studies demonstrate either no effect of diameter on the deteriorated HTC or a small increase in HTC with an increase in diameter.

Similar to the diameter effect, another important parameter which is affecting heat transfer is the pressure. The crux of the present paper also inquired about the heat transfer characteristics near-critical pressure and above the critical pressure. Fig. 2 [25] displays a variety of specific heat with respect to temperature at different SC pressures. It is well known that the pseudo-critical temperature, at which specific heat is maximum, increases with an increase in pressure; Nonetheless, the magnitude of maximum specific heat gradually decreases with an increase in pressure. Zhu et al. [25] also manifested that at low heat flux, the HTC decreases with an increase in pressure. Gang et al. [26] revealed that at higher mass flux (G=1000kg/m²s), HTC increased with decreasing Pressure. Then again, at lower mass flux (G=350 kg/m²s), HTC increased with increasing pressure. They suggested that the trend change might be due to the HTD occurring at Pressure 230 bar and mass flux 350 kg/m²s. Recently Shen et al. [27] experimentally verified the same phenomenon as reported in [26]. They discovered that the inside wall temperature increases with an increase of pressure in the pseudo-critical region and the magnitude of the peak in the HTC decrease for heat flux 250 kW/m^2 and mass flux 690 kg/m^{2}s at 285, 300 and 320 bar pressure.

However, massive studies are being carried out in order to gain a better interpret of the heat transfer behavior at supercritical conditions, the phenomena of enhanced heat transfer and deteriorated heat transfer is not understood thoroughly and they depend on multiple factors like fluid pressure and temperature, diameter of the tube, heat flux and mass flux. Notwithstanding, the principal objective is to compute the tube metal temperature. Several empirical equations are being developed (Mokry et al. [11], Dittus-Boelter et al. [28], Bishop et al. [29], Ornatsky et al. [30], Jackson et al. [31] and Xianliang et al. [32]) to calculate the metal temperature. The aforementioned equations are listed in Table 1. These equations are arrived based on dimensionless parameters but the nonlinearity changes of fluid properties near pseudocritical points are difficult to handle by these dimensionless equations.

As an alternative, Loewenberg et al. [33] developed a lookup table to predict the wall temperature in vertical tubes in which supercritical fluid is flowing upward. Totally 5280 data available in the look-up table are obtained by the various experiments. The look-up table covers the mass flux, heat flux, pressure, bulk enthalpy and diameter in the ranges of 700 to 3500 kg/m^{2}s, 300 to1600 kW/m2, 225 to 250 bar, 1200 to 2700 kJ/kg and 8 to 20 mm respectively. The look-up table is easy to apply for the determination of the metal temperature at any given condition.

Numerical investigations are the cheapest approach in order to investigate the supercritical heat transfer behavior. CFD study is applied in order to interpret the flow behavior and variation in temperature along the radial direction of the tube at any cross-section. Since thermo-physical properties drastically change near the pseudocritical region, CFD simulation software is capable of obtaining these properties. Koshizuka et al. [10] performed a 2-D numerical analysis for heat transfer of supercritical water in a 10 mm circular tube and compared the numerical results with the experimental data of Yamagata et al. [16]. It was discovered that both the

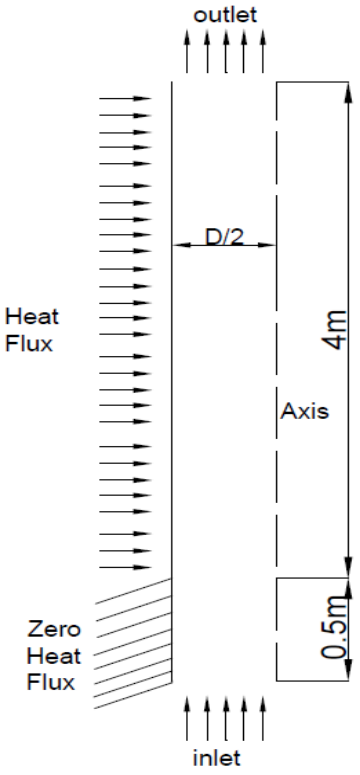

Figure 3. Computational geometry

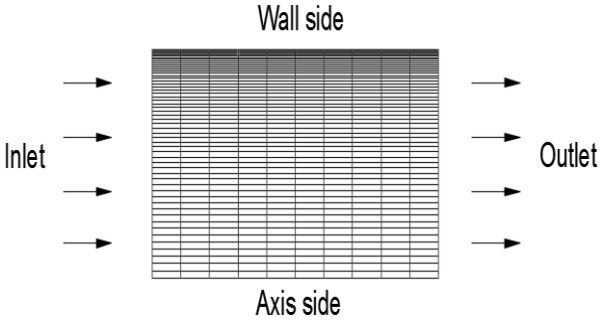

Figure 4. Zoomed view of the computational mesh

numerical result and experimental results are perfectly matching. However, standard wall functions of the turbulence models are not capable of predicting heat transfer deterioration. Moreover, it was concluded from the literature Jaromin et al. [34] that the SST k-ω model is capable of predicting heat transfer deterioration close to the experimental results. Wen and Gu [12] also validated a few turbulent models and reported that SST k-ω is more accurate than other models. Zhia et al. [35] employed an SST k-ω model for predicting convective heat transfer to hydrocarbon fuel at supercritical pressure and assured that it performs well compared to all other turbulence models under supercritical pressure. Zhia et al. [13] applied the SST k-ω model in his analysis and validated with experimental results and exhibited that the SST k-ω model is capable of reproducing the heat transfer enhancement and heat transfer deterioration. In accordance with it, the SST k-ω model is chosen for this present analysis.

The present work aims to explore the effect of heat flux to mass flux ratio, diameter and pressure because these factors are the main cause for heat transfer enhancement and heat transfer deterioration. Tube sizes of 10, 15 & 20 mm inner diameter with 4 m length have been modeled separately and made simulations to study the effect of diameter. The effect of pressure and heat flux is also being investigated for the pressure between 225 and 280 bar and heat flux to mass flux ratio between 0.27 and 0.67.Additionally, a Visual Basic Program code has also been developed to assess the empirical correlations available in the literature in the context of predicting metal temperature with 5280 number of operating conditions.

2. NUMERICAL METHODS

2.1 Geometry

In the present work, the vertical smooth tube of ID 10 mm and length 4 m has been selected for validation for which experimental results are available in the literature (Mokry et al. [11,36]). Consequently, the computational test parameters contemplated in the present work are the same as experiments conducted in Mokry et al. [11,36]. All the simulations in this paper are carried out by applying ANSYS Fluent 17.2. A 2D axis symmetry geometry has been modeled and portrayed in Fig. 3. Since the metal temperature is uniform around the circumference of the vertical tube, a 2D model with axis-symmetry has been chosen for simulation in order to reduce the computational time. To take care of entrance effects, a 0.5m of additional length is also provided without heat flux to make the flow fully developed. The physical boundary conditions of the geometry are as follows: a uniform mass flux with inlet fluid temperature is specified at the inlet and uniform heat flux is employed around the wall boundary for the heated length and zero heat flux is applied on the unheated length of wall boundary. The pressure outlet setting in the Fluent is used as an outlet boundary condition and the symmetry condition is applied for the axis.

2.2 Governing equations

The basic governing equations, including the conservations of mass (the continuity equation), momentum and energy, together with the SST k-ω method is applied in order to simulate the unique and complicated turbulent heat transfer characteristics at supercritical pressure [7].

$$\frac{\partial(\rho u_i)}{\partial x_i} = 0 \tag{6}$$

$$\frac{\partial(\rho u_i u_j)}{\partial x_j} = \rho g_i - \frac{\partial p}{\partial x_i} + \frac{\partial \tau_{ij}}{\partial x_j} + \frac{\partial}{\partial x_j}\left(-\overline{\rho u_i' u_j'}\right) \tag{7}$$

Where $\tau_{ij} = \mu\left(\frac{\partial u_i}{\partial x_j} + \frac{\partial u_j}{\partial x_i} - \frac{2}{3}\delta_{ij}\frac{\partial u_k}{\partial x_k}\right)$

By using Boussinesq approximation, the turbulent shear stress can be found from the following equation in which Reynolds stresses are related to the average velocity gradient

$$-\overline{\rho u_i' u_j'} = \mu_t\left(\frac{\partial u_i}{\partial x_j} + \frac{\partial u_j}{\partial x_i} - \frac{2}{3}\delta_{ij}\frac{\partial u_k}{\partial x_k}\right) - \frac{2}{3}\delta_{ij}\rho k$$

Where $\mu_t$is turbulent viscosity which is flow property; not a fluid property

In the present work, the SST k-ω model is applied as follows:

$\mu_t = \rho\frac{k}{\omega}$

k-$\boldsymbol{\omega}$ equations are derived from transport equations empirically for turbulent kinetic energy(k) and specific dissipation rate (ω) .

$$\frac{\partial}{\partial t}(\rho k) + \frac{\partial}{\partial x_i}(\rho k u_i) = \frac{\partial}{\partial x_j}\left[\Gamma_k \frac{\partial k}{\partial x_j}\right] + G_k - Y_k + S_k \tag{8}$$

And

$$\frac{\partial}{\partial t}(\rho\omega) + \frac{\partial}{\partial x_i}(\rho\omega u_i) = \frac{\partial}{\partial x_j}\left[\Gamma_\omega \frac{\partial \omega}{\partial x_j}\right] + G_\omega - Y_\omega + S_\omega \tag{9}$$

G_k–generation of turbulence kinetic energy as a result to mean velocity gradients, G_ω- generation of turbulence kinetic energy at ω, Y_M and Y_ω– dissipation of k and ω, Γ_k and Γ_ω – effective diffusivity of k and ω, S_k, S_ϵ - user defined source terms.The governing differential equations are solved by applying the finite volume method. The QUICK scheme is employed in order to estimate the convection terms in momentum and energy equations. The SIMPLE procedure is selected to couple pressure and velocity. The algebraic equations are solved with ADI methodology. As mentioned above, fluid properties also abruptly change with pressure and temperature; consequently NIST Refprop which is an inbuilt program in Fluent, has been employed to compute fluid properties. The simulations are stopped when the convergence criteria become less than 10-6 so as to assure enough accuracy level.

2.3 Grid Independence Study and Validation

As the accuracy of results depends consequent to the fineness of the grid, great care is required for selecting the grid size. More fineness of the grid increases the computational time. Therefore, a grid independence study has been demonstrated to select the appropriate size of the grid. Any further refinement of the mesh wouldn't change the solution. The test has been conducted for the geometry shown in Fig.3 with various gird size of 60×1200, 80×1200, 100×1200 100×1200, 120×1200, 140×1200

(radial nodes × axial nodes). Since the change in the parameters in the radial direction is larger than the axial direction, non-uniform nodes with a successive ratio of 1.02 in the radial direction to have dense mesh near the wall and uniform nodes in the axial direction were used. Fig. 4 exhibits the zoomed view of computational mesh to represent fine mesh near the wall and coarse mesh near the axis. The additional 0.5 m length (presented in Fig. 3) is separately divided in to 120×300 grid nodes. In order to choose the appropriate mesh, simulation has been employed for the experimental operating condition of Mokry et al. [11] with pressure 241 bar, heat flux 141 kW/m^2, mass flux of 504 kg/m^{2}s with various mesh sizes. The obtained metal temperature for various meshes are plotted and compared with experimental data as manifested in Fig.5. It is found that the temperature plot at 120×1200 and 140×1200 grids closely matches with experimental data. Moreover, any further refinement of mesh does not alter the solution. Therefore, 120×1200 mesh has been selected for all the computations. In order to gain confidence, one more validation has also been carried out for the pressure 241 bar, heat flux 190 kW/m2 and mass flux 498 kg/m2s. Metal temperature is plotted against the length of the tube and compared with experimental metal temperature of Mokry et al. [36] represented in Fig.6. This indicates that the present simulation model is appropriate.

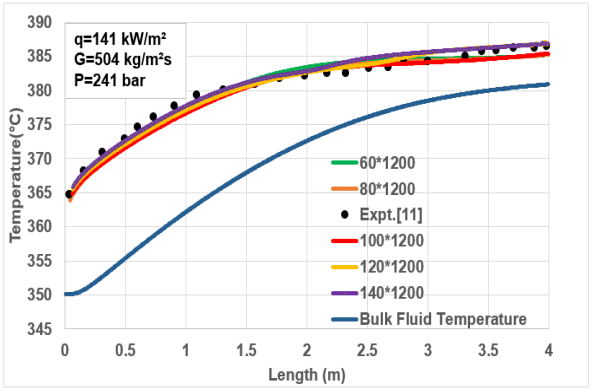

Figure 5. Grid Independence Study for q =141 kW/m² G=504

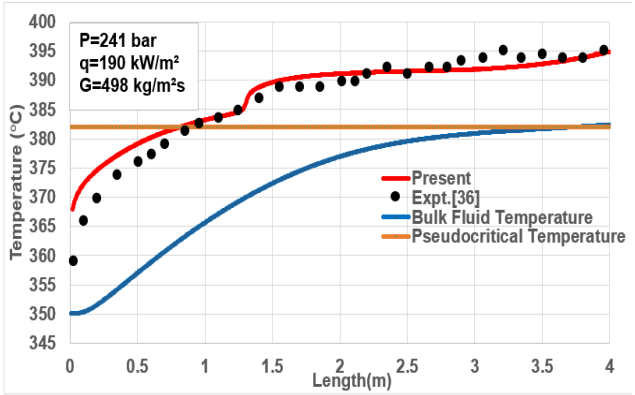

Figure 6. Validation of present numerical simulation with experimental result of [36] q =190 kW/m² G=498 kg/m²s.

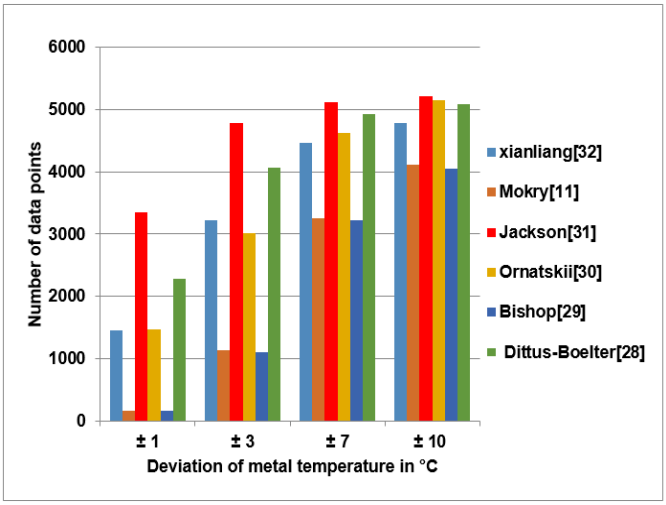

Figure 7. The number of data points deviated in Centigrade for the prediction of metal temperature by various correlations with lookup table data.

3. RESULTS AND DISCUSSION

3.1 Assessment of Empirical Correlations

There are several empirical correlations developed to predict the metal temperature at supercritical conditions. However, these correlations have their own limitations according to the experiment range it has been conducted. Moreover, the accuracy towards the prediction of metal temperature declines particularly near the pseudocritical region due to the non-linear changes in the thermophysical properties. In order to assess the correlations, a Visual basic program code has been developed to predict metal temperature applying the six correlations presented in Table 1. Furthermore the code developed is capable of predicting the fluid properties at supercritical conditions. The developed code was run for 5280 operating conditions to predict metal temperature applying the six correlations and compared with lookup table data of [33]. The assessment of these correlations was ranked based on the deviations ± 1˚C, ± 3˚C, ± 7˚C, ±10˚C with lookup table data and illustrated in Table 2. This deviation is also represented through the histogram as depicted in Fig.7. It indicates that 4777 numbers of data were within ± 3˚C predicted by Jackson correlation when compared to other correlations. This reveals that Jackson correlations predict well; however, it also displays significant deviations with more than ± 7˚C for around 500 data points. This may be a result of the non-linear variation of fluid properties in the pseudocritical region. Deviations of wall temperatures measured by the six correlations compared with lookup table data are tabulated in terms of percentage is presented in Table 3. It is found that 90% of data are within ± 3% deviation when predicted by Jackson correlation. In general, empirical correlations are not very accurate to predict the metal temperature at all ranges of conditions. Therefore, a numerical approach shall be the best alternative to predict the metal temperature and

Table 1 Significant Correlations available in the Literature

SL.No	Researcher	Correlation	Validity Range
01	Dittus-Boelter(1930)[28]	$Nu = 0.023Re^{0.8}\,Pr^{0.4}$	0.7≤Pr≤160 Re ≥101000 $L/D_{hyd} \geq 10$
02	Bishop(1964)[29]	$Nu = 0.0069Re^{0.9}\,\overline{Pr}^{0.66}\left(\frac{\rho_w}{\rho_b}\right)^{0.43}\left(\frac{\overline{Cp}}{Cp_b}\right)^{0.613}$	P=234-293 bar T_b = 282 – 527 °C G= 651 – 3662kg/m^{2}s q= 310 – 3460 kW/m^2
03	Ornatskii(1971)[30]	$Nu = 0.023Re^{0.8}\,Pr_{min}^{0.8}\left(\frac{\rho_w}{\rho_b}\right)^{0.3}$	Pr_{min} - minimum of Pr_bor Pr_w. P=226-294 bar, q= 400-1810 kW/m^2 G= 450 -3000 kg/m^{2}s Inlet enthalpy=420 – 3000 kJkg^{-1} d= 3 mm
04	Jackson(2002)[31]	$Nu = 0.0183Re^{0.82}\,Pr^{0.5}\left(\frac{\rho_w}{\rho_b}\right)^{0.3}\left(\frac{\overline{Cp}}{Cp_b}\right)^{n}$ (4) $n = 0.4$ for $T_b < T_w < T_{PC}$ and $1.2T_{PC} < T_b < T_w$ $n = 0.4 + 0.2\left(\frac{T_w}{T_{PC}} - 1\right)$ for $T_b < T_{PC} < T_w$ $n = 0.4 + 0.2\left(\frac{T_w}{T_{PC}} - 1\right)\left(1 - 5\left(\frac{T_b}{T_{PC}}\right) - 1\right)$ for $T_{PC} < T_b < 1.2T_{PC}$	P=228 -276 bar d=1.6 – 20mm G=700 – 3600 kg/m^{2}s 46<q<260 kW/m^2 $8x10^4$<Re_b<$5x10^5$ 0.85<$\overline{Pr}$<65 0.9 <$\frac{\rho_w}{\rho_b}$<1 0.02<$\frac{\overline{Cp}}{Cp_b}$< 4
05	Mokry(2010)[11]	$Nu = 0.0061Re^{0.904}\,\overline{Pr}^{0.684}\left(\frac{\rho_w}{\rho_b}\right)^{0.564}$	P=240 bar T_b = 320-350 °C G= 200 – 1500 kg/m^{2}s q= 1250 kW/m^2
06	Xianliang(2018)[32]	$Nu = 0.0072Re^{0.891}\,Pr^{0.6}\left(\frac{\rho_w}{\rho_b}\right)^{0.49}$	$4.27x10^3$<Re<$7.4x10^6$ 0.57<Pr<8.5 0.09<$\frac{\rho_w}{\rho_b}$<0.93

Table.2. No. of data points deviated in °C with 5280 Lookup table data.

	No of outputs within the range of the deviation					
Deviation	**Xianliang Lei[32]**	**Mokry[11]**	**Jackson[31]**	**Ornatskii[30]**	**Bishop[29]**	**Dittus-Boelter[28]**
± 1 ℃	1450	164	3343	1466	164	2280
± 3 ℃	3216	1137	4777	3020	1108	4075
± 7 ℃	4464	3262	5115	4617	3225	4928
± 10 ℃	4783	4107	5213	5151	4048	5094

Table 3. No. of data points deviated in % with 5280 Lookup table data.

	No of data points %			
Correlation	± 1 %	± 3 %	± 7 %	± 10 %
Bishop[29]	3.11	20.98	61.08	76.67
Mokry[11]	3.11	21.53	61.78	77.78
Xianliang Lei[32]	27.46	60.91	84.55	90.59
Ornatskii [30]	27.77	57.2	87.44	97.56
Dittus–Boelter[28]	43.18	77.18	93.33	96.48
Jackson[31]	63.314	90.47	96.875	98.73

Table 4. Parameters simulated in the present work for the study of heat flux to mass flux ratio.

S.no	Pressure, bar	Heat flux (q)kW/m^2	Mass flux (G) (kg/ m^2 s)	q/G ratio (kJ/kg)
1	241	134	499	0.27
2	241	180	499	0.36
3	241	234	499	0.47
4	241	334	499	0.67

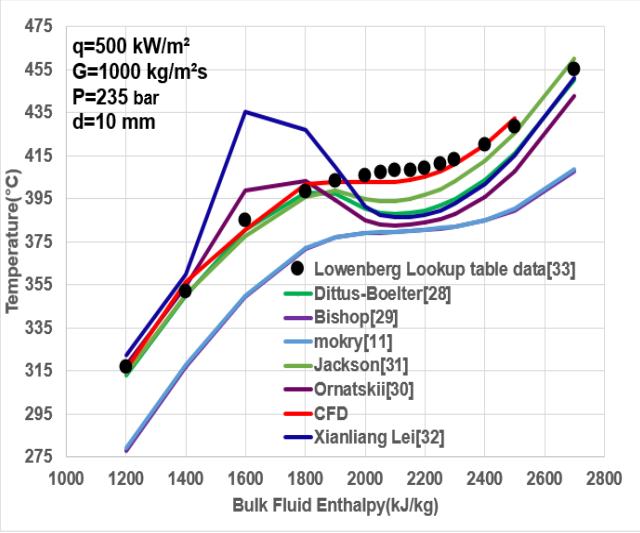

Figure 8. Comparison of wall temperature obtained by CFD, Lookup table and correlations

understanding the heat transfer phenomenon. A case study of mass flux 1000 kg/m²s, heat flux 500 kW/m², pressure 235 bar and inner diameter 10 mm has been selected from lookup table simulated applying CFD tool. The wall temperature obtained by CFD is compared with the metal temperature of lookup table data and of various correlations and depicted in Fig. 8. It is manifested that CFD results exactly match with look-up table data compared to correlations results.

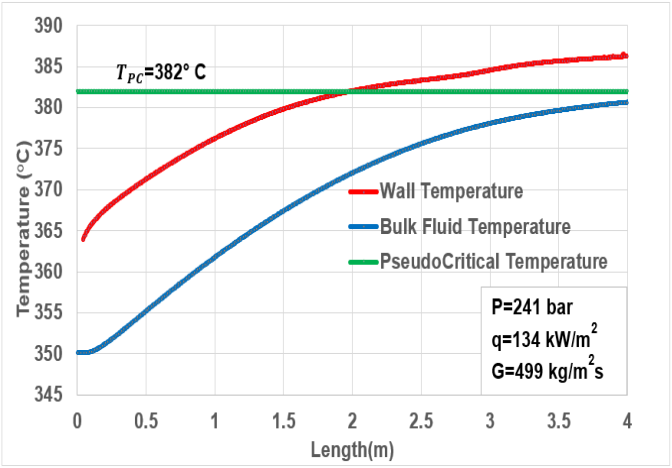

Figure 9. Wall temperature along the length of the tube for q/G=0.27kJ/kg, q =134 kW/m² G=499 kg/m²s.

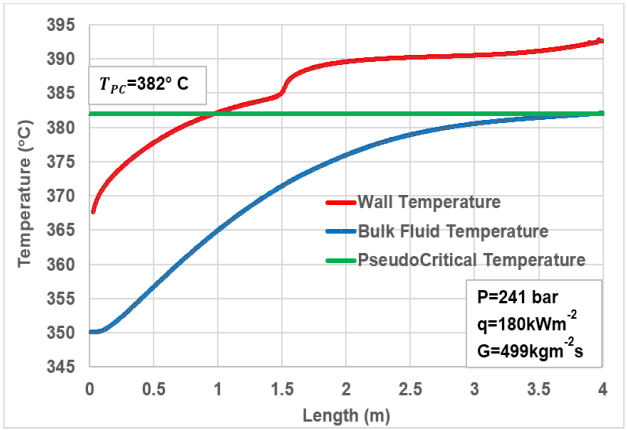

Figure 10. Wall temperature along the length of the tube for q/G=0.36kJ/kg, q =180 kW/m², G=499 kg/m²s.

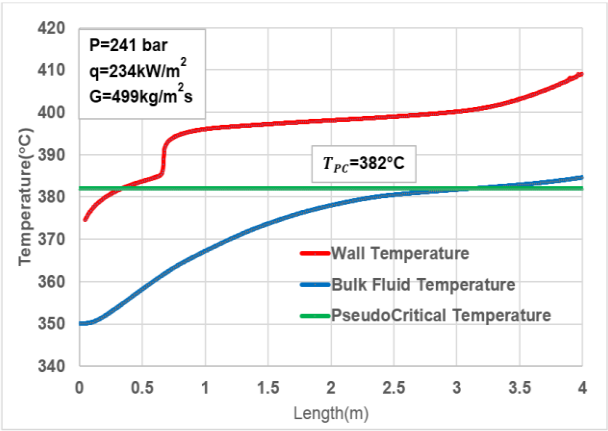

Figure 11. Wall temperature along the length of the tube for q/G=0.47kJ/kg, q =234 kW/m², G=499 kg/m²s.

3.2 Effect of Heat Flux to Mass Flux ratio

In the present work, the behavior of the heat transfer phenomenon at supercritical conditions has been analyzed. Like boiling crisis phenomenon in subcritical conditions, heat transfer deterioration is observed in supercritical conditions. Unlike subcritical conditions, supercritical heat transfer deterioration is not due to critical steam

quality. It depends on heat flux to the mass flux ratio. The present study investigates the effect of heat and mass flux ratio. Table 4 represents the various heat flux to mass ratio analyzed in the present work. The range selected to examine the heat flux to the mass flux ratio is 0.27 to 0.67. For all the cases, the pressure is kept as a 241 bar for which the pseudocritical temperature is 382oC. Figs.9 to 12 represent the temperature plot simultaneously the length of the tube for various values of heat flux to mass flux ratio. In Fig.9 corresponding to q/G = 0.27 (heat flux = 134 kW/m2 and mass flux = 499 kg/m2s), it is clearly observed that the dissimilarity between wall temperature and the bulk temperature is decreasing along the length of the tube. This phenomenon is heat transfer enhancement where the heat transfer coefficient keeps on increasing in conformity of the length of the tube. Therefore, there is a decreasing trend in the slope of the wall temperature. Fig.10 corresponds to q/G = 0.36 (heat flux = 180 kW/m2 and mass flux = 499 kg/m2s). It is revealed that there is a small sudden jump in wall temperature. Fluid in contact with the wall reaches pseudocritical temperature and the fluid at the core is less than pseudocritical temperature. This indicates that the fluids near the wall are low-density fluid and the fluids at the core are high-density fluid. At pseudocritical temperature, the thermal conductivity of the fluid decreases. Hence, the sudden jump in wall temperature may be due to the low thermal conductivity of the fluid near the wall. Fig.11 corresponds to q/G = 0.47 (heat flux = 180 kW/m2 and mass flux = 234 kg/m2s). It is notably observed in Fig.11 that the magnitude of a sudden rise in wall temperature increases when compared to the rise in temperature observed in Fig.10. Moreover, it manifested that as the wall temperature reaches pseudo critical temperature, a shoot-up exists in wall temperature and the magnitude of the rise in wall temperature depends on the value of heat flux to mass flux ratio. This type of heat transfer phenomenon is heat transfer deterioration. The dissimilarity between wall temperature and bulk fluid temperature increases which leads to heat transfer deterioration behavior. Furthermore, Sharabi and Ambrosini [37] concluded that as heat flux to mass flux ratio increases, buoyancy starts to play a role in the heat transfer mechanism causing a degradation effect that can outbalance the heat transfer enhancement due to the large specific heat. Fig.12 corresponds to q/G = 0.67 (heat flux = 334 kW/m2 and mass flux = 499 kg/m2s). It is observed that there is a sudden rise in temperature around 70℃, which is obviously a heat transfer deterioration phenomenon. Such a sudden rise in temperature should be avoided in the evaporator panels of supercritical boilers. The zoomed portion of the temperature contours when the bulk fluid temperature reaches pseudocritical temperature is displayed in Fig. 13a and 14a for q/G 0.27 and q/G 0.67 respectively. It represents the change in temperature between the wall and fluid. The temperature profile along the radial direction for q/G 0.27 and q/G 0.67 is presented in Fig 13b and Fig. 14b as well. It is clearly observed that for q/G 0.27, temperature change between the wall and fluid is only 10℃ as a result of heat transfer enhancement and for q/G 0.67, temperature change between the wall and fluid is 70℃ because of heat transfer deterioration. The wall temperature computed by numerical simulation and corresponding available experimental data are compared as well. Though CFD is not able to predict the exact magnitude of the rise in temperature, it favorably gives direction to the design engineers. When the q/G ratio is more, the mixed effect of buoyancy and thermal acceleration increases or the heat transfer deterioration increases and lowers the heat transfer performance.

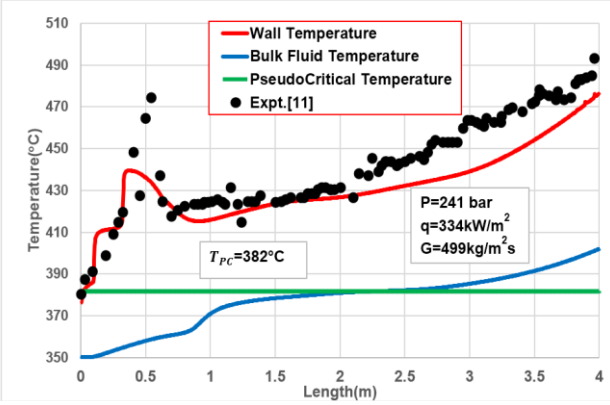

Figure 12. Wall temperature along the length of the tube for q/G=0.67kJ/kg, q =334 kW/m², G=499 kg/m²s.

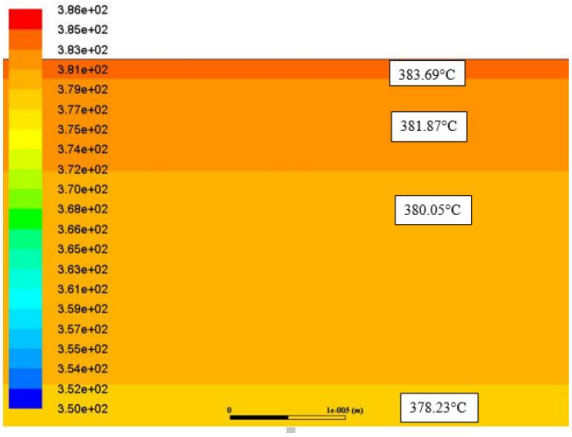

Figure 13a. Zoomed portion of the temperature contour in the radial direction at x=2m of q/G=0.27kJ/kg

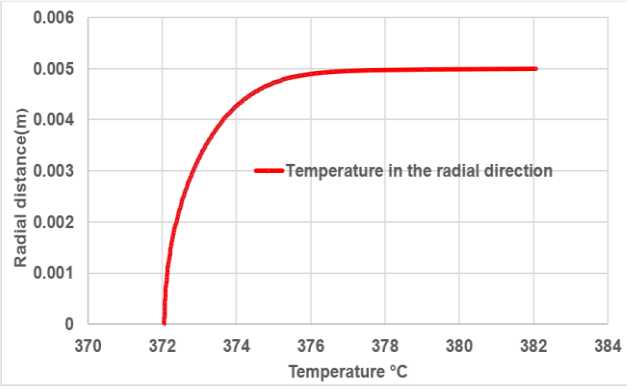

Figure 13b. Temperature distribution in Radial direction at x=2m of q/G=0.27kJ/kg.

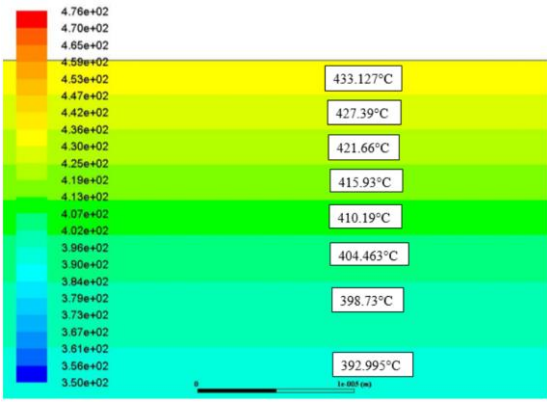

Figure 14a. Zoomed portion of the temperature contour in the radial direction at x=0.5m of q/G=0.67kJ/kg.

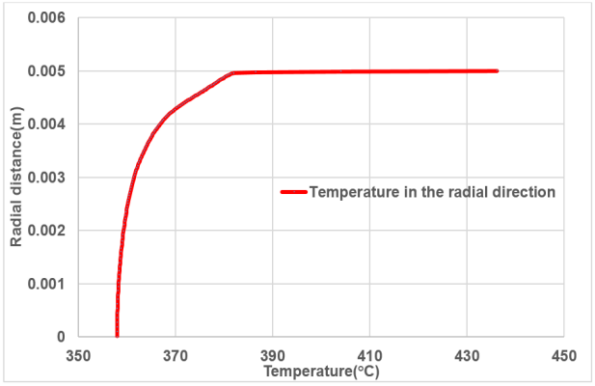

Figure 14b. Temperature distribution in Radial direction at x=0.5m of q/G=0.67kJ/kg.

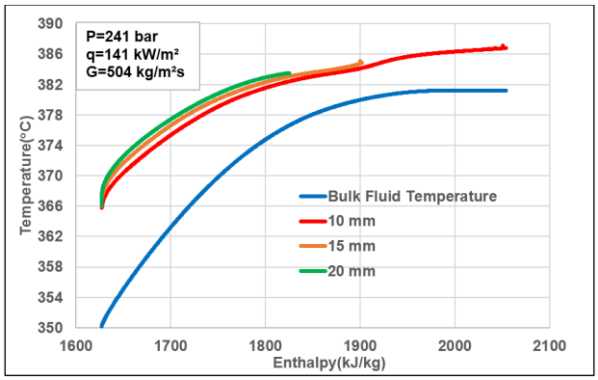

Figure 15a. Effect of diameter on heat transfer by Wall temperature at the q=141kWm² and G=504 kg/m²s

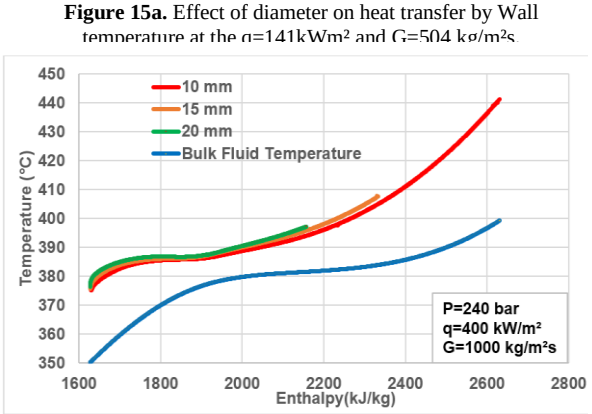

Figure 15b. Effect of diameter on heat transfer by Wall temperature at the q=400kW/m², G=1000 kg/m²s.

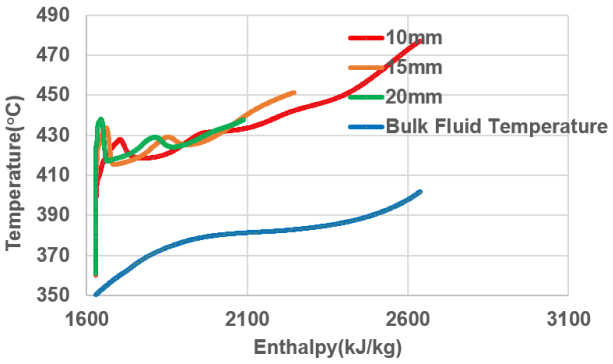

Figure 15c.Effect of diameter on heat transfer by Wall temperature at the q=334kW/m², G=499 kg

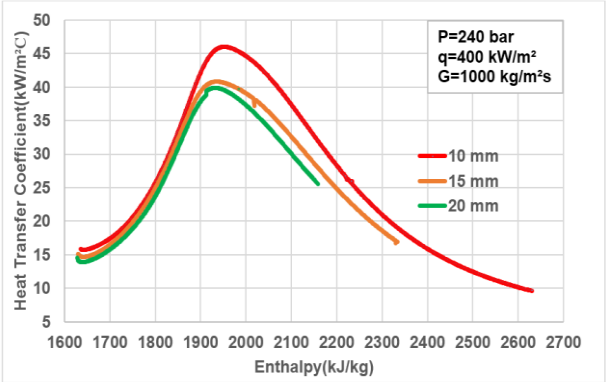

Figure 16a. Effect of diameter on heat transfer by HTC at the q= 141kW/m², G= 504 kg/m²s.

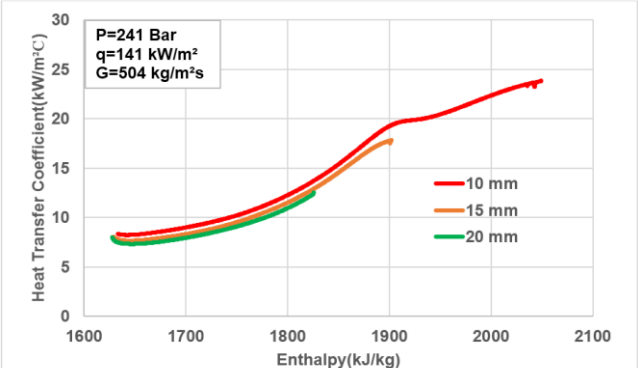

Figure 16b. Effect of diameter on heat transfer by HTC at the q=400kW/m²and G=1000kg/m²s.

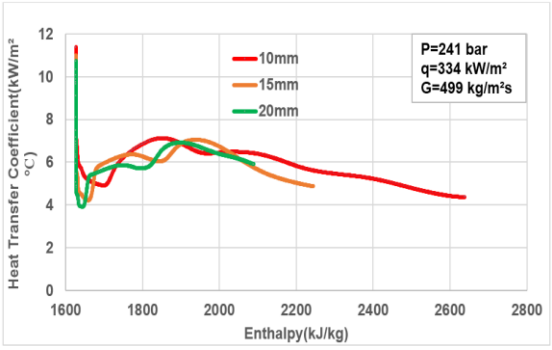

Figure 16c. Effect of diameter on heat transfer by HTC at the q=334kW/m², G=499kg/m²s.

3.3 Effect of diameter on heat transfer

The present work covers the investigation of heat transfer behavior at various diameters of the tubes. Since the q/G ratio is one of the key factors for HTD, the effect of diameter has been analyzed at low q/G and high q/G. The case I as displayed in Table 5, is investigated for various inner diameters of 10, 15 and 20 mm at pressure 241 bar at lower q/G of 0.27. The reason for selecting these parameters is that Mokry et al. [11] conducted an experiment for the tube of 10 mm diameter with q=141 kW/m² G=504 kg/m²s at 241 bar. The comparison of the present result with the experiment is exhibited in Fig 6. Case II & III shown in Table 5 are for the same parameters at higher q/G of 0.4 and 0.67 respectively. The wall temperature and HTC plotted against bulk fluid enthalpy for various diameters for the Case I, Case II and Case III are highlighted in Fig. 15a-c and 16 a-c respectively. It was observed that as the diameter increases, the wall temperature also increases or the heat transfer coefficient in smaller diameter tubes is higher than in larger diameter tubes. At q/G 0.67, HTD has appeared for all 10, 15 and 20 mm diameter tubes with the highest magnitude of the rise in temperature for a larger diameter. Buoyancy plays a key role in the onset of HTD. For the same flow conditions, the effect of buoyancy is stronger for larger diameter tubes which could delay the onset of HTD for smaller diameter tubes. At high q/G, when Tb<Tpsc<Tw, a M shaped velocity profile is observed as a result of a larger change in density between the wall and the bulk fluid which can generate stronger buoyancy effect (Ref. Fig. 17 and Fig. 18). The increase in the thickness of the low-density layer (supercritical steam whose thermal conductivity is lower) near the wall retards the heat transfer from the wall to the fluid which causes the HTD. Then again, at low q/G =0.27, a logarithmic velocity profile has been observed where no effect of buoyancy has been seen. The change in density between the wall and fluid is small and hence the fluid is capable of absorbing the heat from the wall because of the high thermal conductivity of the fluid near the wall.

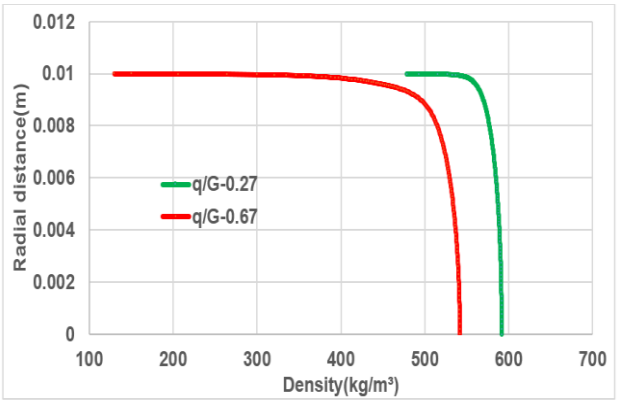

Figure 17. Density variation in the radial direction at x=1.5m for q/G 0.27 and q/G 0.67.

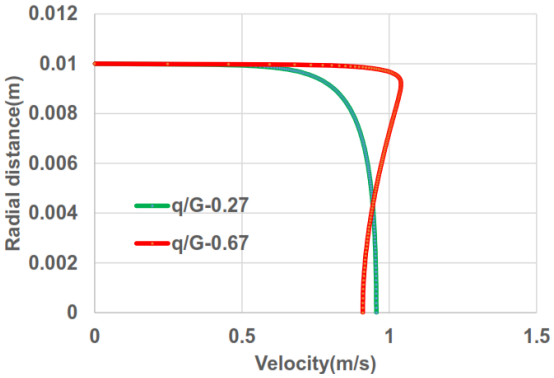

Figure 18. Velocity variation in the radial direction at x=1.5m for q/G 0.27 and q/G 0.67.

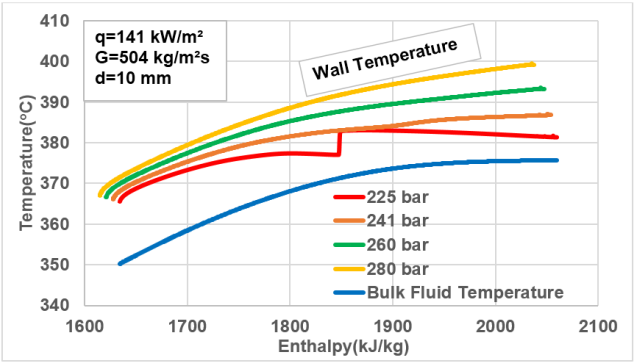

Figure 19 a. Effect of Pressure on heat transfer by Wall temperature at the q=141kW/m², G= 504 kg/m²s and d=10 mm.

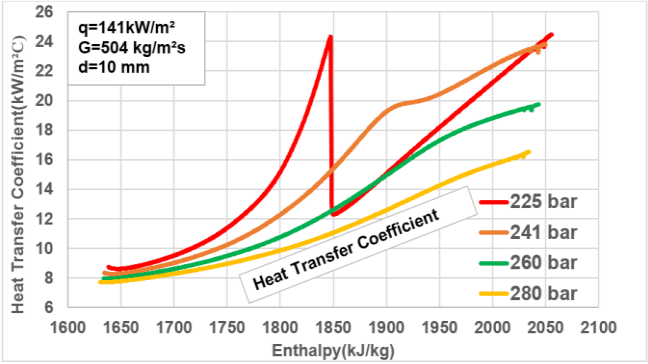

Figure 19 b. Effect of Pressure on heat transfer by HTC at the q= 141 kW/m², G= 504 kg/m²s and d=10mm

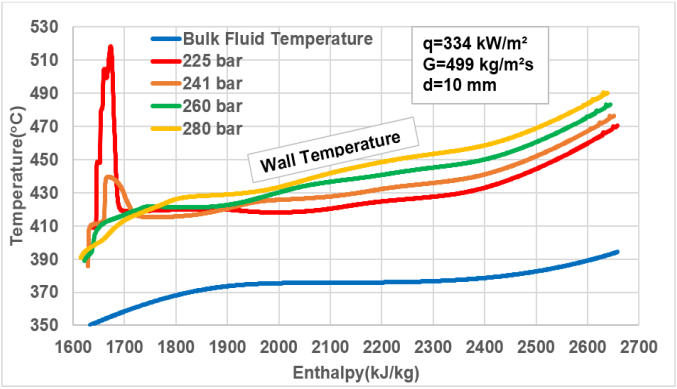

Figure 20 a. Effect of pressure on heat transfer by Wall temperature at the q=334kWm-2and G=499 kg/m²s.

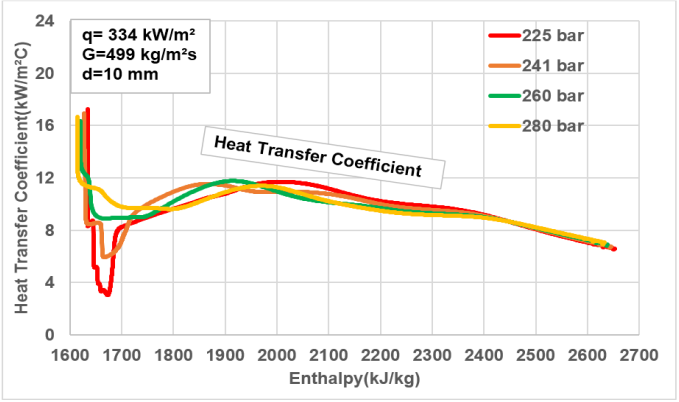

Figure 20 b. Effect of Pressure on heat transfer by HTC at the q= 334 kWm2 and G= 499 kg/m²s.

3.4 Effect of pressure on heat transfer

Furthermore, the present work covers the investigation of heat transfer behavior at various SC pressures. Like the previous case, the effect of pressure is also inquired for a lower q/G ratio of 0.27 and a higher q/G ratio of 0.67, as presented in Table 6. In Case I, a heat flux of 141 kW/m²and mass flux of 504 kg/m²s and in case II a heat flux of 334kW/m²and mass flux of 499 kg/m²s have been chosen to inquire the heat transfer behavior for the pressures of 225,240,260 and 280 bar in 10 mm diameter tube. The variations in the wall temperature and HTC against bulk fluid enthalpy under different pressures for q/G = 0.27 are displayed in Fig. 19a-b. It is observed that as the pressure increases, the wall temperature increases as well. This implies that the degree of HTE decreases with an increase in pressure. It is referred from Fig. 2 that the magnitude of the rise in specific heat decreases with an increase in pressure. Furthermore, it is one of the reasons for the increase in wall temperature with pressure. It is also observed that the HTC reduces from 24.48 to 16.52 kW/m²C as pressure increases from 225 to 280 bar. Fig.20 a-b indicates the variations in the wall temperature and HTC against bulk fluid enthalpy under different pressures for q/G =0.67. As depicted in Fig. 21, peak wall temperature attains maximum at 225 bar and it decreases with an increase in pressure. It is observed that HTD occurs at 225 bar and 240 bar and no evidence of HTD at 260 bar and 280 bar exists. Moreover, the trend of wall temperature is reversed i.e., at lower q/G, as pressure increases wall temperature also increases and at higher q/G, as pressure increases wall temperature decreases. It coincides with the report by Gang et al. [26] and Shen et al. [27].

4. Conclusions

This paper numerically investigates the effect of heat and mass flux ratio, diameter and pressure when supercritical water flows in a vertical smooth tube. All the simulations were carried out applying ANSYS-Fluent 17.2 version. A proper grid independency study has been employed in order to select the appropriate mesh and carefully validated with experimental results. A Visual basic program has been developed to access the metal temperature prediction of various empirical correlations and ranked based on the deviation with experimental data. It was discovered that empirical correlations have limitations and significantly deviate when Tb < Tpsc < Tw. CFD is capable of predicting the metal temperature at all conditions with minimal deviations. Numerical investigations were employed for the mass flux range of 500 – 1000 kg/m²s, heat flux range of 100 - 500 kW/m2, a pressure range of 225 to 280 bar and inside diameter 10, 15 and 20 mm. The heat flux to mass flux ratio varied between 0.27 to 0.67 such that a low ratio leads to heat transfer enhancement and a high ratio leads to heat transfer deterioration. It was found that heat transfer enhancement was observed at q/G = 0.27, where the difference between wall temperature and bulk fluid temperature decreases in accordance with the length of the tube. A heat transfer deterioration phenomenon was observed from q/G=0.36 onwards; however the magnitude in the rise in temperature depends on the value of q/G. For q/G=0.36, the sudden rise in wall temperature was only 10oC but for q/G 0.67, the sudden rise of 70oC temperature was observed. The effect of inside diameter was inquired for 10, 15 & 20 mm and found that the probability for the occurrence of heat transfer enhancement decreased with an increase in diameter. Buoyancy parameter is the main criterion for the onset of heat transfer deterioration. For the same flow conditions, it is found that the effect of buoyancy is stronger for larger diameter tubes. At high q/G, when Tb < Tpsc < Tw, an M-shaped velocity profile is observed as a result of a larger change in density between the wall and the bulk fluid which can generate stronger buoyancy effect. The study about the effect of pressure clears that at low q/G ratio 0.27, the chances of heat transfer enhancement decreases with increase in pressure. Alternatively, at a higher q/G ratio of 0.67, the magnitude of the sudden rise in wall temperature (heat transfer deterioration) decreases with an increase in pressure. The heat transfer deterioration was observed for 225 and 240 bar which is near the critical point and no HTD was observed at 260 and 280 bar. Therefore, boilers operated far away from critical pressure are safer than operating near critical pressure for the same q/G ratio. It is found that CFD is capable of predicting HTD and can be applied as a replacement for conducting experiments. While designing the evaporator panel of SC boilers, higher diameter tubes, and high q/G ratio at the vicinity of critical pressure should be avoided, as it leads to failure of water wall tubes due to the high probability of HTD.

References

[1] US DOE Nuclear Energy Research Advisory Committee and Generation IV International Forum, A Technology Roadmap for

Table 5. Parameters simulated in the present work for the study of diameter analysis

SL.NO	Inside Diameter (mm)	CASE I (q/G=0.27)		CASE II (q/G=0.4)		CASE III (q/G=0.67)	
		Heat flux (q) kW/m^2	Mass flux (G) (kg/ m^2 s)	Heat flux (q) kW/m^2	Mass flux (G) (kg/ m^2 s)	Heat flux (q) kW/m^2	Mass flux (G) (kg/ m^2 s)
1	10	141	504	400	1000	334	499
2	15	141	504	400	1000	334	499
3	20	141	504	400	1000	334	499

Table 6. Parameters simulated in the present work for the study of pressure analysis

SL.NO	Pressure (bar)	CASE I(q/G=0.27)		CASE II(q/G=0.67)	
		Heat flux (q) kW/m^2	Mass flux (G) (kg/ m^2 s)	Heat flux (q) kW/m^2	Mass flux (G) (kg/ m^2 s)
1	225	141	504	334	499
2	240	141	504	334	499
3	260	141	504	334	499
4	280	141	504	334	499

Generation IV Nuclear Energy Systems, (2002).

[2] M.W. Shitsman, Heat transfer to SC helium, carbon dioxide, and water: Analysis of thermodynamic and transport properties and experimental data, Cryogenics, 14 (2), 77–83 (1974).

[3] H. Griem, A new procedure for the prediction of forced convection heat transfer at near- and SC pressure, Heat and Mass Transfer, 31 (5), 301–305 (1996).

[4] S.K. Yang and H.F. Khartabil, Normal and deteriorated heat transfer correlations for SC fluids, Transaction of the American Nuclear Society, November 13–17, Washington, D.C., USA, 93, 635–637 (2005).

[5] X. Lei, H. Li, W. Zhang, T. Dinh, Y. Guo, S. Yu, Experimental study on the difference of heat transfer characteristics between vertical and horizontal flows of supercritical pressure water, Applied Thermal Engineering, 113, 609–620 (2017).

[6] J J. Wang, H. Li, S. Yu, T. Chen, Comparison of the transfer characteristic of SC pressure water to that of subcritical pressure water in vertically-upward tubes, Int. J. Multiphase Flow, 37, 769–776 (2011).

[7] M. K. Rowinski, J. Zhao, T. J. White, Y. Ch. Soh, Numerical investigation of supercritical water flow in a vertical pipe under axially non-uniform heat flux, Progress in Nuclear Energy 97, 11-25 (2017).

[8] X. Cheng, T. Schulenberg, D. Bittermann, P. Rau, Design analysis of core assembly for supercritical pressure conditions. Nucl. Eng. Des. , 223, 279–294 (2003).

[9] R. B. Duffey, I. Pioro, X. Zhou, U. Zirn, S. Kuran, H. Khartabil, M. Naidin Supercritical Water-Cooled Nuclear Reactors (SCWRs): current and future concepts – steam cycle options Icone 16, Proceeding of the 16th International Conference on Nuclear Engineering, 4, 469–477 (2008).

[10] S. Koshizuka, N.Takano, Y. Oka, Numerical analysis of deterioration phenomenon in heat transfer tosupercritical water. Int. J. Heat Mass Transfer, 38, 3077–3084 (1995).

[11] S. Mokry, I. Pioro, A. Farah, K. King,S. Gupta, W. Peimana, P. Kirillov, evelopment of supercritical water heat-transfer correlation for vertical bare tubes Nuclear Engineering and Design, 241, 1126–1136, (2011).

[12] Q. L. Wen, H. Y. Gu, Numerical simulation of heat transfer deterioration phenomenon in supercritical water through vertical tube. Annals of Nuclear Energy, 37, 1272–1280 (2010).

[13] Z. Shen, D. Yang, S.Wang, W.Wang,Y. Li, Experimental and numerical analysis of heat transfer towater at supercritical pressures, International Journal of Heat and Mass Transfer, 108, 1676–1688 (2017).

[14] S. Anand, S. Suresh, D. Santhoshkumar, Numerical study for the effect of heat and mass flux on heat transfer characteristics of supercritical water flows in a upward vertical tube Proceeding of the 24thNational and 2nd International ISHMT-ASTFE Heat and mass transfer conference (IHMTC-2017)BITS Pilani, Hyderabad, India December, 27-30 (2017).

[15] S. Anand, S. Suresh, D. Santhoshkumar, Numerical study for the effect of diameter and pressure on heat transfer characteristics of supercritical water flows in a upward vertical tube International conference on Numerical Heat transfer and

fluid flow NIT Warangal, India- Jan19-21 (2018).
[16] K. Yamagata, K. Nishikawa, S. Hasegawa, Forced convective heat transfer to SC water flowing in tubes, Int. J.Heat Mass Transfer, 15 , 2575– 2593 (1972).
[17] J. W. Ackerman, Pseudo-boiling heat transferto supercritical pressure water in smooth and ribbed tubes, Trans. ASME, 490–498 (1970).
[18] R. A. Lee, K. H. Haller, SCwater heat transfer developments, and applications Proc. 5th International Heat Transfer Conference, Japan, 4(7), 335–339 (1974).
[19] J. H. Song, H.Y. Kim, H. Kim, Y.Y. Bae, Heat transfer characteristics of a SC fluid flow in a vertical pipe, J. Supercrit.Fluids, 44,164–171 (2008).
[20] M. J. Watts, C. T. Chou, Mixed convection heat transfer to SC pressure water, Proceedings of the 7th International Heat Transfer Conference, Munich, Germany, 495–500 (1982).
[21] T. Yamashita, S. Yoshida, H. Mori, S.Morooka, H. Komita, K. Nishida, Heat transfer study under SC pressure conditions, ENES4/ANP2003, Kyoto, JAPAN, 11-19 (2003).
[22] D. Jackson, W. D. Haller, Influences ofbuoyancy on heat transfer to fluids flowing in vertical tubes under turbulent conditions, Turbulent Forced Convection in Channels and Rod Bundles, 2, 613–640 (1979).
[23] Y. Y. Bae, H. Y. Kim, D.J. Kang, Forced and mixed convection heat transfer to SC CO2 vertically flowing in a uniformly-heated circular tube, Exp. Thermal Fluid Sci., 34 , 1295–1308 (2010).
[24] S. Yildiz, Groeneveld Diameter effect on SC heat transfer International Communications in Heat and Mass Transfer, 54, 27–32 (2014).
[25] B. Zhu, Ch. Yang, An investigation on heat transfer characteristics of different pressure steam-water in vertical upward tube, Nuclear Engineering and Design, 239, 381–388 (2009).
[26] B. Gang, W. Yang, H. Zhu, Experimental investigation of heat transfer for SC pressure water flowing in vertical annular channels, Nuclear Engineering and Design, 241, 4045– 4054 (2011).
[27] Shen, Xie, Nie, Liu, Wang. Flow and Heat transfer characteristics of high-pressure water flowing in a vertical upward smooth tube at low mass flux conditions, Applied Thermal Engineering, 102, 391–401 (2016).
[28] F. W. Dittus and L. M. K. Boelter, Heat Transfer in Automobile Radiators of the Tubular Type, 3rd ed. Publications in Engineering, Berkeley: University of California, 443 (1930).
[29] A. Bishop, R. O. Sandberg, and L. S. Tong, High Temperature Supercritical Pressure Water Loop. Part IV. Forced Convection Heat Transfer to Water at Near-Critical Temperatures and Supercritical Pressures, Pittsburgh, USA: Westinghouse Electric Corp. (1964).
[30] P. Ornatskij, L. F. Glushchenko and S. I.Kalachev, “Heat transfer with rising and falling flows of water in tubes of small diameter at supercritical pressures,” Therm. Eng., 18(5), 137–141 (1971).
[31] J. D. Jackson, “Consideration of the heat transfer properties of supercritical pressure water in connection with the cooling of advanced nuclear reactors,” in: Proceedings of the 13th pacific Basin Nuclear Conference, Shenzhen City, China, October 21–25 (2002).
[32] X. Lei, Y. Guo, W. Zhang, H. Li and L. Li Development of Heat Transfer Correlation for Supercritical Water in Vertical Upward Tubes heat transfer engineering, (2018).
[33] M. F. Loewenberg, E. Laurien, A. Class, T. S. Berg, Supercritical water heat transfer in vertical tubes: A look-up table Progress in Nuclear Energy, 50, 532-538 (2008).
[34] M. Jaromin, H. Anglart, A numerical study of heat transfer to supercritical water flowing upward in vertical tubes under normal and deteriorated conditions. Nuclear Engineering and Design, 264, 61– 70 (2013).
[35] T. Zhi, Ch. Zeyuan, Z. Jianqin, L. Haiwang, Effect of turbulence models on predicting convective heat transfer to hydrocarbon fuel at supercritical pressure.Chinese Journal of Aeronautics, 29 (5), 1247–1261 (2016).
[36] M. Pioro, K. Gospodinov, SC water heat transfer in a vertical bare tube, Nuclear Engineering and Design, 240, 568–576 (2010).
[37] M. Sharabi, W. Ambrosini, Discussion of heat transfer phenomena in fluids at supercritical pressure with the aid of CFD models, Annals of Nuclear Energy, 60-71 (2009).